

**High Average Power Laser Program  
Optics and Chamber Studies**  
*2005 Progress Report*

**M. S. Tillack, F. Najmabadi, A. R. Raffray,  
K. Cockrell, Z. Dragojlovic, R. Harrison, A. Iroezi,  
R. Martin, J. E. Pulsifer, K. Sequoia and X. Wang**

**5 February 2006**



# **High Average Power Laser Program Optics and Chamber Studies *2005 Progress Report***

M. S. Tillack, F. Najmabadi, A. R. Raffray,  
K. Cockrell, Z. Dragojlovic, R. Harrison, A. Iroezi,  
R. Martin, J. E. Pulsifer, K. Sequoia and X. Wang

**5 February 2006**

## **Abstract**

This report describes the results of research performed at UC San Diego in support of the High Average Power laser program. Our research focuses on the prediction of chamber and optic responses in inertial fusion energy (IFE) power plants and simulation of those phenomena through modeling and scaled experiments. Progress occurred in four primary topical areas: (1) Laser-induced damage to grazing-incidence metal mirrors, (2) Chamber wall materials response to pulsed loading by x-rays and high-energy ions, (3) Chamber design studies, and (4) IFE chamber dynamics and clearing following target explosions.

## **Outline**

Task 1: Optics Damage and System Integration Studies

- 1.1. Statement of purpose
- 1.2. Background
- 1.3. Progress report

Task 2: Experimental Studies of Laser-IFE Chamber Armor

- 2.1. Statement of purpose
- 2.2. Progress report

Task 3: Design studies for the Laser-IFE Fusion Chamber

- 3.1. Statement of purpose
- 3.2. Progress report

Task 4: Chamber Dynamics and Clearing

- 4.1. Statement of Purpose
- 4.2. Progress report

# Task 1: Optics Damage and System Integration Studies

## 1.1. Statement of purpose

Our research seeks to create a better understanding of damage mechanisms, to develop acceptable materials and designs, and to demonstrate the performance characteristics of final optics for laser IFE. Through both experimentation and modeling we will determine limitations on the operation of reflective optics for IFE power plants under prototypical environmental conditions. Commercially available optics are not capable of meeting the stringent requirements on damage resistance; therefore, a major element of this research is the development of materials and fabrication techniques that will provide reliable, long-lived optics for fusion energy. This activity involves interactions with industrial vendors to help develop practical, scalable technologies. We work collaboratively with other HAPL organizations to define specific final optic design concepts and key interfaces in a laser-IFE power plant, and to field both small and medium scale prototypes for testing in HAPL facilities.

## 1.2. Background

In any laser fusion system, the final optics for each beamline are located in the direct line-of-sight of the exploding fusion targets. Consequently, that optic is exposed to a variety of damage threats. These include prompt neutron and gamma fluxes, x-ray and ion emissions, and “long” time-scale threats from condensable target and chamber materials. The potential consequences include increased laser absorption, degradation of the beam quality, and reductions in the laser-induced damage threshold (LIDT). In addition to the “final optic”, the upstream “penultimate optic” may experience significant neutron fluences. This optic is expected to be a dielectric mirror, such that neutron damage to dielectric materials and multi-layer coatings must be addressed.

Three primary goals for damage resistance have been specified previously [1.1]. We require that the optics operate for 2 years ( $>10^8$  shots) at an incident fluence level of  $5 \text{ J/cm}^2$  normal to the beam. In-situ reconditioning is allowed if it can be accomplished without significantly degrading the plant availability. The maximum tolerable level of damage corresponds with 1% increased absorption and degradation of the wavefront by  $\lambda/3$  ( $\lambda=248 \text{ nm}$  for KrF). An increase in absorption equivalent to 1% of the incident beam is likely to result in laser-induced damage to the optic as well as degradation of the spatial profile and increased difficulty balancing the power amongst many beams. The wavefront degradation limit was chosen based on two important target illumination constraints: the spatial nonuniformity of the beam on target must be less than 1% and the spot size and position must be known to within 20 microns. As a rule of thumb, surface aberrations of the order of  $\lambda/3$  will lead to a doubling of the propagation parameter  $M$  [1.2], which corresponds to a doubling of the diffraction-limited spot size and a doubling of the beam divergence. The allowable wavefront distortion in the final optic depends on the allocation of wavefront distortions throughout the entire optical path as well as the margin for error. Pending further guidance on the precise wavefront requirements on target, we are using  $\lambda/3$  as our goal.

Our primary emphasis during Phase I of the HAPL program has been on grazing incidence metal mirrors. This concept was proposed in 1991 as an alternative to dielectric multilayer mirrors due to expectations that neutron damage would be far less serious, thereby reducing the need for expensive radiation damage testing [1.3]. As a result of this perceived advantage, the concept of a GIMM was also adopted in the Prometheus and Sombrero power plant studies [1.4,1.5].

During the past three years, we have addressed many of the issues for GIMM's, including manufacturing techniques, laser damage threshold, and protection against debris and x-rays. Progress is described in Section 1.3. The primary emphasis on further GIMM studies involves the use of more prototypical pulse conditions, end-of-life demonstrations, large-scale (10 cm) mirror fabrication and testing, and system integration. In addition, we propose to contribute to efforts on neutron irradiation damage to both GIMM's and multilayer dielectrics (for the final or penultimate optic). Our proposal for future work is presented in Section 1.4.

### **1.3. Progress report**

During the past 3 years, under grants from the Naval Research Laboratory, we have obtained grazing incidence metal mirrors from several vendors, performed damage testing at 248 nm, and characterized the surfaces both before and after exposure using a variety of surface analysis techniques. In the following two subsections we review progress on (a) mirror development and (b) laser-induced damage testing.

#### *(a) Mirror development*

Our studies have highlighted the importance of purity, microstructure and coating characteristics on damage. For example, damage morphology is clearly related to grain size, and so techniques to produce smaller grains have been explored. A common method of fabricating amorphous metal mirrors is by thin film deposition. Unfortunately, conventional thin film deposition techniques are capable of only limited coating thickness, of the order of 200 nm. Our studies have shown that the coating thickness is a critical parameter for damage resistance, and that values over 10  $\mu\text{m}$  offer significant advantages. Therefore, we have embarked on a mirror development program to create new kinds of high-damage threshold metal coatings.

Our two most successful mirror fabrication techniques have been electroplating and "thick" evaporative coating. In both cases, the resulting surfaces must be post-processed in order to provide optical quality. We have tried both polishing and diamond turning. Processing of pure aluminum is notoriously difficult; to date, no vendor has been able to produce acceptable polished surfaces. However, we have identified three vendors capable of meeting power plant specifications using diamond turning. All of the processes under investigation are scalable.

Figure 1 shows two electroplated, diamond-turned optics prior to exposure. Mirror 83 exhibits little grain structure, whereas the micrograph of mirror 80 indicates significant grain structure, with grain size of the order of 20 microns. Note, the contrast evident in the figures should not be interpreted as an indication of surface height morphology. Surface profiling of both of these mirrors indicates an rms roughness of only 5 nm. Contrast under optical microscopy strongly depends on lighting conditions, which in this case were optimized to highlight surface features.

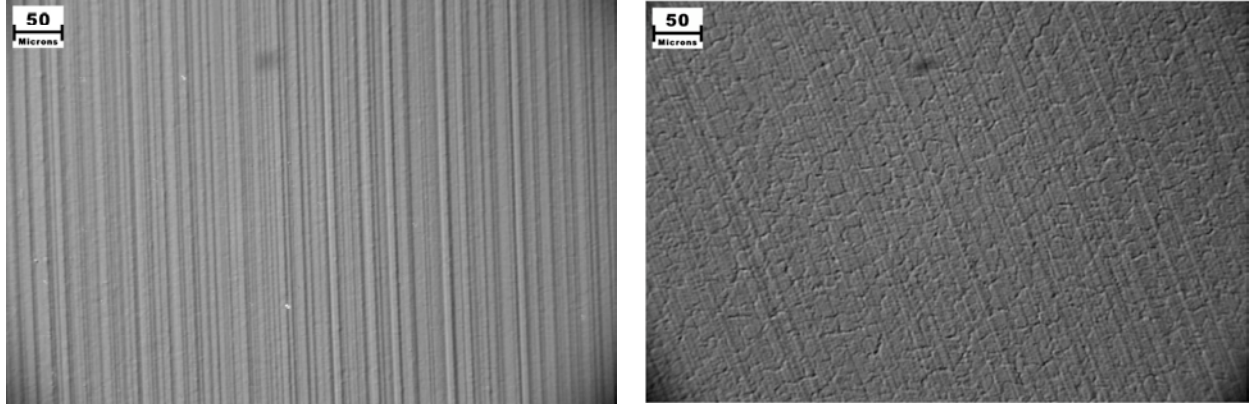


Figure 1. Surface morphology of electroplated mirrors. (a) mirror 83, (b) mirror 80

*(b) LIDT testing*

We have acquired extensive data on electroplated aluminum using our laboratory excimer laser with 25-ns pulse length. Fluence levels were scaled to maintain the same peak surface temperature expected in a power plant. At 10 Hz, we were able to achieve up to  $10^6$  shots on specimens. Mechanisms of damage depend not only on the surface microstructure, but also the fluence level. Our data suggest two damage pathways: rapid onset (at high fluence, low shot count) and cumulative growth (at low fluence, high shot count). Figure 2 shows examples of these two pathways. The optical micrograph for rapid onset exhibits a localized highly damaged site, whereas the micrograph for cumulative growth shows a gradual destruction of the entire surface due to grain boundary motions.

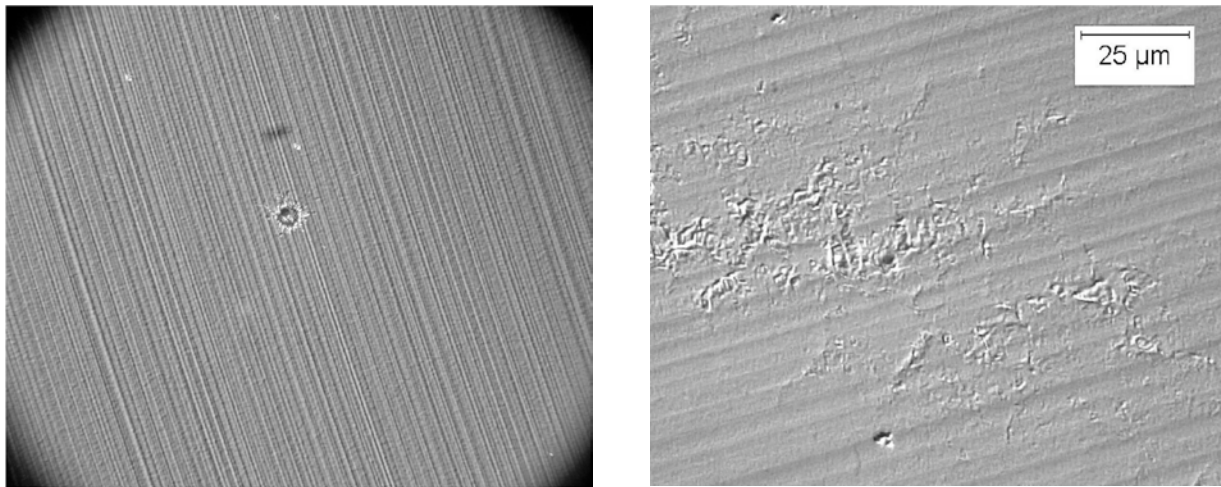


Figure 2. Pathways for mirror damage. (a) rapid onset, (b) cumulative growth

Damage curves were created for electroplated mirrors, demonstrating that they can achieve the power plant goal fluence. Figure 3 plots the results from many exposures on two mirror surfaces. Each data point represents the number of shots at a given fluence level when the surface damage has exceeded a level at which catastrophic failure is imminent. We determine this condition based on visual observation of light emitted from the surface due to dark-field

backlighting (with a HeNe laser) as well as fluorescence emitted by the excimer beam interacting with the aluminum.

To date, we have not been able to acquire data to end-of-life values ( $3 \times 10^8$  shots). In Figure 3 we extrapolate by applying the commonly-used power law:

$$F_2/F_1 = (n_2/n_1)^{s-1}$$

Depending on the surface quality, as evidenced in Figure 1, the exponent  $s$  is either 0.915 or 0.955. Using a 25-ns pulse length, our goal fluence is  $10 \text{ J/cm}^2$ . As seen in the figure, the better mirror achieves this, but the safety factor is marginal.

Based on our observations of the morphology of damage, we believe that better results would be obtained if the grain size could be further reduced. We have probably reached the limit of electroplating. Therefore, we have begun to develop and test thick e-beam coatings. In addition, we have installed a 100-Hz excimer laser that will allow us to approach end-of-life testing.

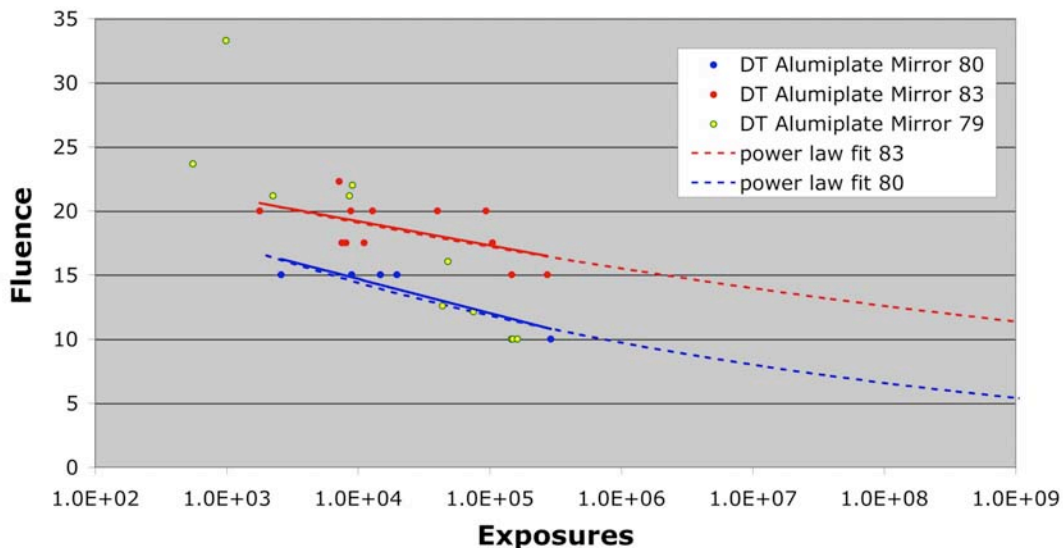


Figure 3. Fluence curves for electroplated mirrors exposed to 25-ns pulses at 248 nm

### References for Task 1:

- 1.1 M. S. Tillack, S. A. Payne, N. M. Ghoniem, M. R. Zaghoul and J. F. Latkowski, "Damage threats and response of final optics for laser-fusion power plants," 2nd Int. Symp. on Inertial Fusion Science and Applications, Kyoto Japan, Sept. 2001.
- 1.2 C. D. Orth, S. A. Payne, and W. F. Krupke, "A Diode Pumped Solid State Laser Driver for Inertial Fusion Energy," *Nuclear Fusion* **36** (1996) 75-116.
- 1.3 R. L. Bieri and M. W. Guinan, "Grazing Incidence Metal Mirrors as the Final Elements in a Laser Driver for Inertial Confinement Fusion," *Fusion Technology* **19** (May 1991) 673-678.
- 1.4 L. M. Waganer, "Innovation Leads the Way to Attractive IFE Reactors – Prometheus-L & Prometheus-H," IAEA Technical Committee Meeting and Workshop on Fusion Reactor Design and Technology, 13-17 Sept. 1993.
- 1.5 "OSIRIS and SOMBRERO Inertial Fusion Power Plant Designs: Final Report," DOE/ER-54100, WJSA-92-01, March 1992.

## **2. Task 2: Experimental studies of laser-IFE chamber armor**

### **2.1. Statement of Purpose**

Our research aims at developing and fielding simulation experiments of laser-IFE chamber armor in order to ensure that all relevant phenomena are taken into account and to benchmark modeling predictions.

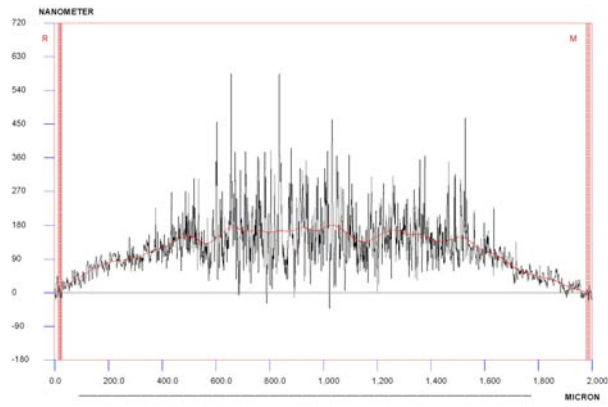
### **2.2. Progress Report**

A laser-IFE chamber wall should accommodate x-ray, ion, and neutron spectra from target explosions and provide the required lifetime. As a source with an integrated and fully prototypical spectrum of x-rays and ions is not available, experiments should be performed in simulation facilities. Our analysis indicates that most of phenomena leading to the failure of the wall depend on wall temperature evolution (temporal and spatial) and chamber environment; only sputtering and radiation (ion & neutron) damage effects depend on “how” the energy is delivered. As such, we proposed to use a laser to generate similar wall temperature and temperature gradients in laser-IFE chamber wall sample. To this end, under a grant from the Naval Research Laboratory, we designed and built a simulation experimental facility, Dragonfire, to determine the thermo-mechanical response of the chamber wall. The facility includes:

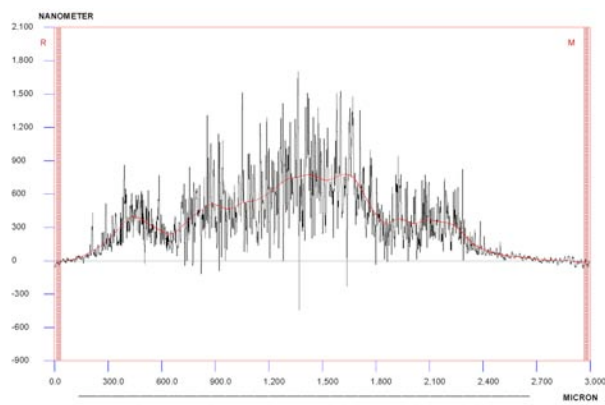
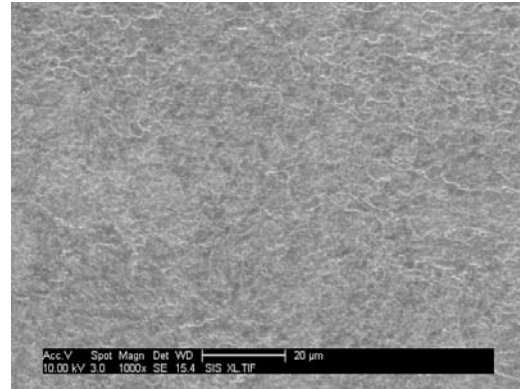
- 1) A 2-J (at 1 micron) Nd-YAG laser which can operate at 10-Hz allowing rep-rated experiments ( $10^6$  shots per day), if necessary.
- 2) A high-temperature sample holder that can maintain the equilibrium sample temperature from room temperature to 1,200 °C.
- 3) A fast optical thermometer with nanosecond resolution, which was developed at UCSD. We have used fiber optics technology to simplify the optical train.
- 4) RGA and micro-balancing systems to measure material loss from samples.

Our fast optical thermometer is an important part of our experiments. During the last period, we fielded the thermometer. At its present mid-gain setting, the thermometer can measure the temperature range of  $\sim 1,500$  to  $\sim 3,500$  K, which is the range of interest for the High-Average-Power Laser program. (The thermometer has a maximum gain of about 5,000 to 10,000, mid-gain refers to values of a few hundred). The thermometer has a temporal resolution of about 1 ns. On the test stand (uniform surface temperature), it has a temperature resolution of a few percent ( $< 3\%$ ). We have calibrated our thermometer using the Optronics UL-45U lamp. We calibrate the thermometer at ONE temperature (for example, 3,000 K) and check the calibration against 6 more calibration points (the Optronics UL-45U lamp we use comes with 7 calibration points at 7 different temperatures). We checked this setup with an electronic flash lamp and we measured 5,500 K, which is the correct color temperature of an electronic flash lamp.

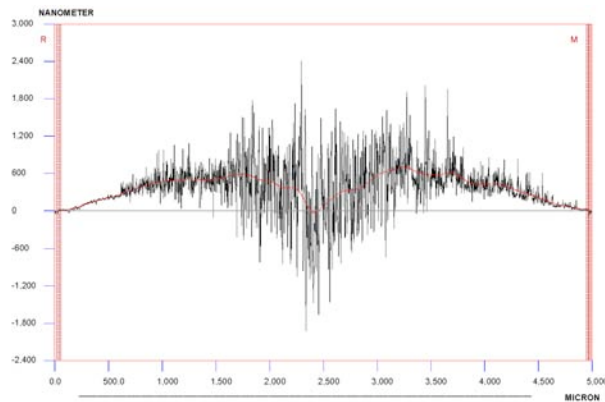
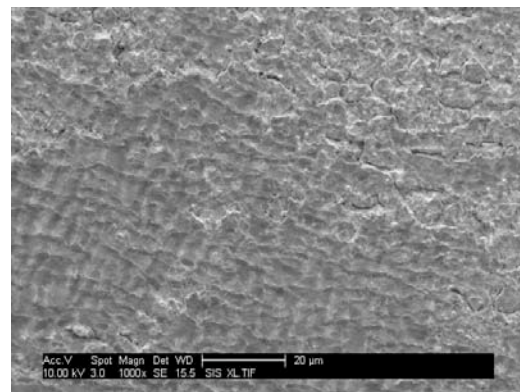
We performed initial long-term exposure tests and surface analysis of the samples for a variety of laser energies and shot rates ( $10^3$  to  $10^5$ ). Some example results are shown in Fig. 2.1



$10^3$  shots



$10^4$  shots



$10^5$  shots

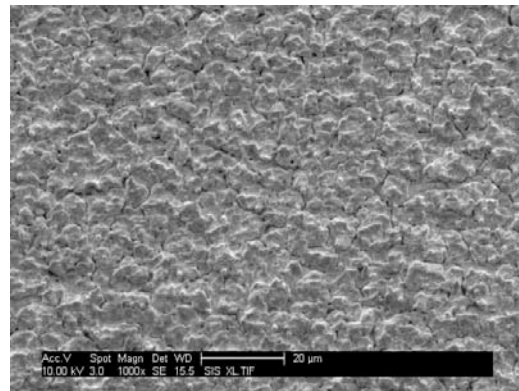


**Fig 2.1.** SEM and Profilometry of W samples irradiated with 240 mJ (equilibrium temperature of 600C and final temperature of 3500C) at three different shot rates.

### **3. Task 3: Design studies for the Laser-IFE Fusion Chamber**

#### **3.1. Statement of Purpose**

The HAPL program is in the later stage of the first phase aimed at developing the critical science and technologies, which will then lead to the next phase of development and integration of full size components. One of the key remaining challenges in Phase I is the development of a concept for a chamber first wall that can repetitively withstand the blast of X-rays, ions and neutrons from the target. The preferred first wall concept is based on tungsten as armor and ferritic steel as structural material. Tungsten has a high melting temperature and well understood material properties. However, armor survival is a key concern that is being investigated. Specific issues are associated with the W armor thermo-mechanical behavior under high heat flux transients, to the integrity of the W/FS bond under prototypical conditions, and to the consequences of He ion implantation. The chamber design should integrate the armor and structural material choices with a blanket concept providing attractive features of design simplicity, fabrication, maintainability, safety and performance (when coupled to a power cycle). This will help in providing an attractive end product for laser IFE. The reference concept is a large chamber design (of radius ~1.5-11 m) with a target yield of ~350 MJ. Advanced concepts (including magnetic intervention) that could result in smaller less costly chambers, better armor survival and lower cost of electricity are also being investigated.

#### **3.2. Progress Report**

Over the last year, UCSD's contribution in this area included armor analysis, chamber design with magnetic intervention, blanket design and analysis for the large chamber, as well as coordination of the chamber tasks. Results of the work have been described in detail through presentations at the three HAPL workshops during 2005 and through presentations at international conferences and publications throughout the year (listed below). Highlights of UCSD's contribution are provided in the next subsections.

##### Presentations at the HAPL workshops:

- 3.W.1 (a) Effect of Cusp Field on Ion Energy Deposition;  
(b) Ion Collector Options for Magnetic Diversion Chamber Concept, presented by A. R. Raffray, HAPL Workshop, Naval Research Laboratory, Washington, D.C., March 3-4, 2005, available at <http://aries.ucsd.edu/HAPL/MEETINGS/0503-HAPL/program.html>
- 3.W.2 Assessment of Blanket Options for Magnetic Diversion Concept, presented by A. R. Raffray, HAPL Workshop, Naval Research Laboratory, Washington, D.C., March 3-4, 2005, available at <http://aries.ucsd.edu/HAPL/MEETINGS/0503-HAPL/program.html>
- 3.W.3 Overview of Chamber/Blanket work, presented by A. R. Raffray, HAPL Workshop, Lawrence Livermore National Laboratory, Livermore, CA, June 20-21, 2005, available at <http://aries.ucsd.edu/HAPL/MEETINGS/0506-HAPL/program.html>
- 3.W.4 Status of the large (reactor) chamber and blanket work, presented by A. R. Raffray, HAPL Workshop, University of Rochester's Laboratory for Laser Energetics, Rochester, NY, 8-9 November 8-9 2005, available at <http://aries.ucsd.edu/HAPL/MEETINGS/0511-HAPL/program.html>

- 3.W.5 Blanket considerations for smaller chambers, presented by A. R. Raffray, HAPL Workshop, University of Rochester's Laboratory for Laser Energetics, Rochester, NY, 8-9 November 8-9 2005, available at <http://aries.ucsd.edu/HAPL/MEETINGS/0511-HAPL/program.html>
- 3.W.6 "Engineering Analysis" of He Retention & Release Experiments to Determine Desirable Engineered W Armor Microstructure, A. R. Raffray, HAPL Workshop, University of Rochester's Laboratory for Laser Energetics, Rochester, NY, 8-9 November 8-9 2005, available at <http://aries.ucsd.edu/HAPL/MEETINGS/0511-HAPL/program.html>

#### Conference Presentations and Papers:

- 3.P.1 A. R. Raffray, J. Blanchard, J. Latkowski, F. Najmabadi, T. Renk, J. Sethian, S. Sharafat, L. Snead and the HAPL Team, "Progress Towards Realization of a Laser IFE Solid Wall Chamber," *Fusion Engineering & Design*, in press, 2006 (presented at ISFNT-7, Japan, 2005).
- 3.P.2 J. D. Sethian, Rene Raffray, Jeff Latkowski, Jake Blanchard, Lance Snead, T. Renk and S. Sharafat, "Considerations for the Chamber First Wall Material in a Laser Fusion Power Plan," *Journal of Nuclear Materials*, **347** (3), 161-177, December 2005.
- 3.P.3 A. R. Raffray and the HAPL Team, "Threats, Design Limits and Design Windows for Laser IFE Dry Wall Chambers," *Journal of Nuclear Materials*, **347** (3), 178-191, December 2005.
- 3.P.4 R. Raffray, J. Blanchard, A. E. Robson, D. V. Rose, M. Sawan, J. Sethian, L. Snead, I. Sviatoslavsky, and the HAPL Team, "Impact of Magnetic Diversion on Laser IFE Reactor Design and Performance," 4<sup>th</sup> International Conference on Inertial Fusion Science and Applications, Biarritz, France, September 5-9, 2005.
- 3.P.5 M.E. Sawan, I.N. Sviatoslavsky, A. R. Raffray, and X. Wang, "Neutronics Assessment of Blanket Options for HAPL Laser Fusion Energy Chamber," to appear in Proceedings of the 21<sup>th</sup> IEEE/NPSS Symposium on Fusion Engineering, Knoxville, TN, September 26-29, 2005.
- 3.P.6 I. N. Sviatoslavsky, A. R. Raffray, M. E. Sawan, and X. Wang, "A Lithium Self-Cooled Blanket for the HAPL Conceptual Inertial Confinement Reactor," *Fusion Science & Technology*, **47** (3), 535-539, April 2005.

#### 3.2.1 Chamber Armor

In order to avoid issues linked with a chamber gas (in particular its impact on target survival and injection), the HAPL program is currently focusing on chambers without a protective gas. This leads to rather large chambers as emerged from the results of a parametric study to determine the combination of chamber size and Xe protective gas density required to maintain the W armor below a maximum temperature limit of 2,400° C (assumed as a preliminary W lifetime criterion). More details can be found in publications 3.P.1 and 3.P.2 listed above. The results are summarized in Figure 3.1 for a 1 mm W armor on a 3.5 mm ferritic steel substrate. A chamber of ~10-11m is required for a 350 MJ yield target (which in combination with a rep rate of ~5 would result in ~1800 MW fusion).

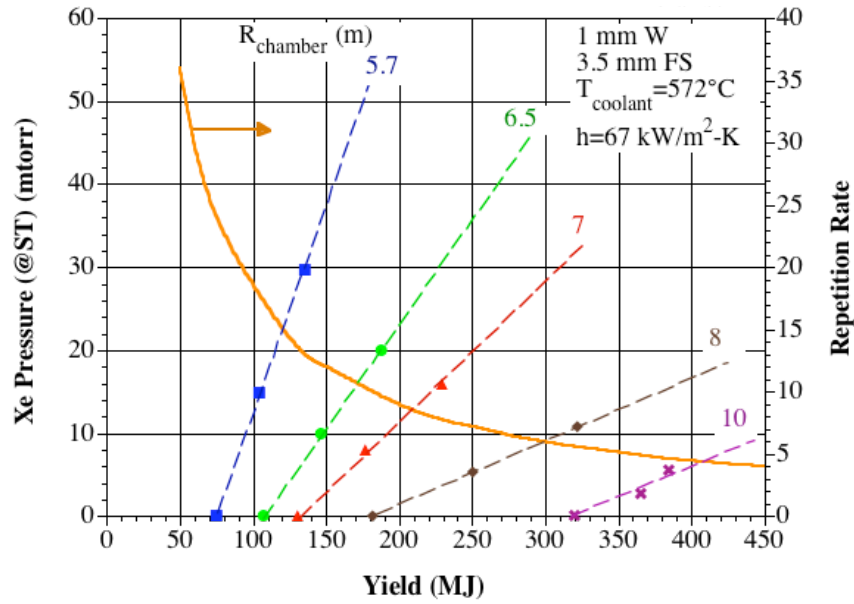


Figure 3.1 Example integrated parametric study showing combinations of chamber gas density (shown as pressure at a standard temperature, ST = 300 K), yield and chamber size that would maintain the W armor temperature  $<2400^{\circ}\text{C}$  for a fusion power of 1800 MW and a coolant temperature of  $572^{\circ}\text{C}$ . The corresponding repetition rate for 1800 MW fusion is shown on the other vertical axis.

The ion and photon energy deposition in the W armor of such a large chamber was calculated for a target yield of 350 MJ, and was used as input to calculate the resulting W temperature profile histories using the RACLETTE-IFE code (see publications 3.P.1 and 3.P.2 listed above). The results were presented at the November 2005 HAPL workshop (see presentation 3.W.4 listed above) and are summarized in Figures 3.2 and 3.3.

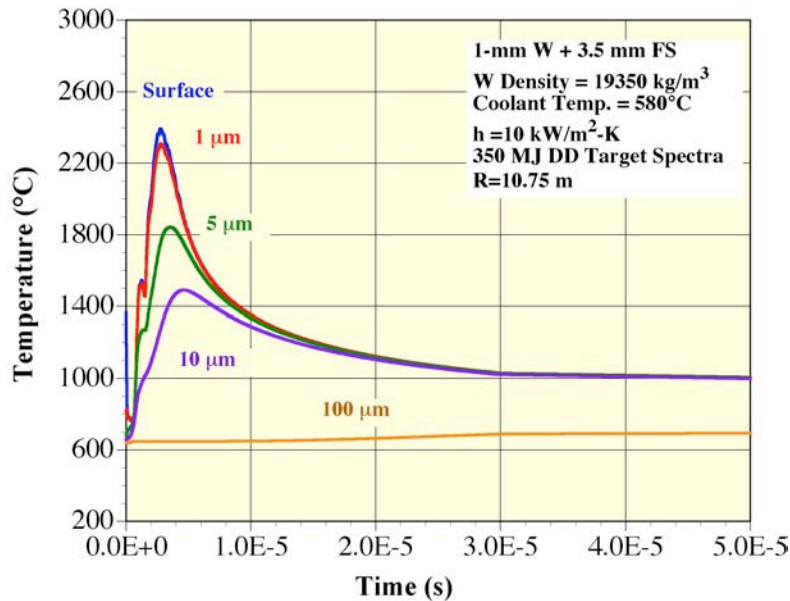


Figure 3.2 W temperature histories at different depths from the surface for the 350 MJ target yield spectra and a 10.75 m radius chamber.

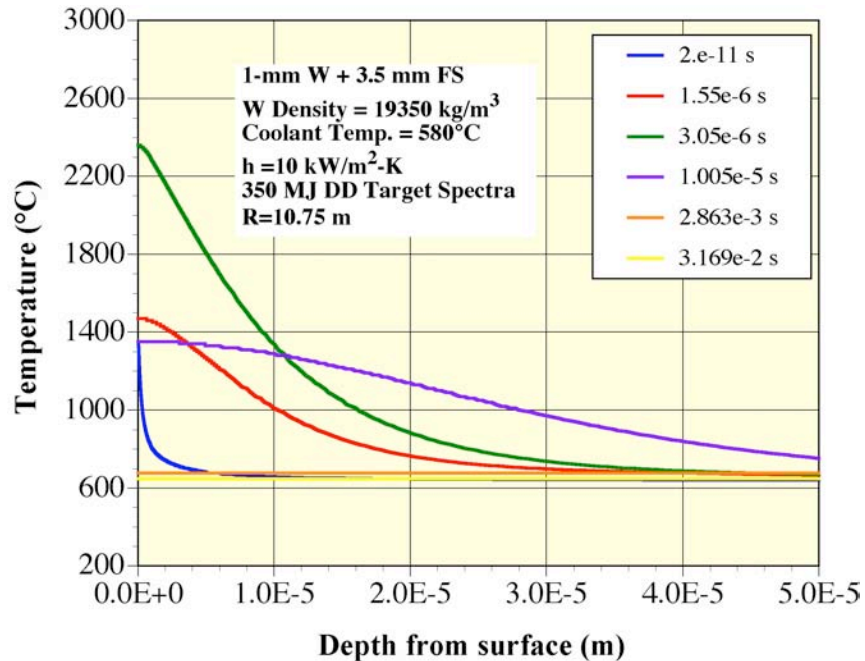


Figure 3.3 W armor temperature gradients at different times following the micro-explosion for a 350 MJ target yield spectra and a 10.75 m radius chamber.

Overall, significant progress has been made by the HAPL team in the understanding of the three major armor issues of long-term thermo-mechanical fatigue, exfoliation due to He ion implantation and ferritic steel/tungsten bonding (see publication 3.P.1 listed above). However, concerns still exist in particular regarding the second issue associated with He implantation. Recent experimental results from the University of North Carolina and Oak Ridge National Laboratory suggest that certain conditions may mitigate the effect of He trapping and bubble formation [3.1]. Less trapping of helium was observed in single crystal tungsten under certain conditions when compared to polycrystalline tungsten from their He implantation and anneal studies. In addition, the results indicate that He retention decreases drastically when a given helium dose is spread over an increasing number of pulses, each one followed by W annealing to 2000°C, to the extent that there would be no He retention below a certain He dose per pulse.

He behavior in W is quite complex as it involves a number of different mechanisms. A simple engineering model was developed at UCSD based on an effective diffusion coefficient (representing a combination of processes) to help understand the experimental results and apply them to prototypical conditions within the experimental parameter range. It is clear that in so doing the activation energy derived from the experiment would not be that of bulk diffusion but of the rate-controlling mechanism (most probably some form of trapping/detrapping mechanisms). The model was used to determine the effective diffusion activation energy required to reproduce the He retention from the experimental results of ref. [3.1]; these results were then used to analyze the IFE case with the prototypical He implantation flux and temperature history (as illustrated in Fig. 3.2). A key question is what atomic fraction of He in W would be acceptable for the W armor to provide the required lifetime. In an earlier presentation, it was suggested that the critical ion/atom concentration for a blister to exfoliate is about 15 at.%

for He in W [3.2]. Based on this, the analysis results suggest that the microstructure characteristic dimension could be somewhat higher than 100 nm. However, given the included assumptions and simplifications in the modeling results presented here and in the absence of more prototypical experimental results, it seems reasonable to maintain the porous tungsten microstructure in the range 50-100nm, which would reduce the He retention to about 0.2-0.8% (normalized to the W atomic concentration). A 10 nm microstructure, if it could be made, would be even better with a fractional He retention of only about  $8 \times 10^{-5}$ . More detail can be found in the HAPL workshop presentation 3.W.6 listed above.

It is important to realize that these results are based on simplifying assumptions. They provide some insight as to the He retention processes and the W microstructure dimension that would help maintain helium retention to an acceptable level. However, the results and related observations must be verified by experiments with engineered material such as those manufactured by PPI (with ~10-15% interconnected porosity and porous microstructure of ~50-100 nm), see HAPL workshop presentation 3.W.6 listed above]. As this work is continuing, it seems prudent to also consider alternatives such as SiC or even innovative ways of accommodating the energy and ion fluxes through phase change for example.

### 3.2.2 Chamber Blanket

The blanket work is a collaborative effort within the HAPL team with major inputs from UCSD (task coordination, conceptual design, CAD work, thermal-hydraulic analysis), UW (conceptual design, overall chamber layout and neutronics analysis) and LLNL (safety and system interface). Interfaces with other relevant components and areas are maintained through close interaction with the experimental armor testing community and the Materials Working Group (MWG).

The effort on the large chamber has included a consistent scoping study of blanket concepts, including a self-cooled lithium blanket, a helium-cooled ceramic breeder blanket, and a dual-coolant lithium lead blanket. UCSD's contribution to this study has been presented at HAPL workshops (see presentations 3.W.3 and 3.W.4 listed above). This has resulted in the selection of a self-cooled lithium blanket with ferritic steel as structural material based on a combination of design simplicity, neutronics performance (see publication 3.P.5 listed above), and reasonable power production when coupled to a Brayton cycle.

The overall chamber layout is illustrated in Figure 3.4. The blanket itself consists of two sets of poloidal modules (upper and lower) with holes for the laser beams, as illustrated in Figure 3.5 (a,b). The blanket design is based on an annular geometry with a first Li pass cooling the walls of the box and a slow second pass flowing back through the large inner channel where the Li is heated to its maximum temperature. A sandwich insulator is used in the inner wall to prevent excessive heat transfer from the hot inner channel to the cooler first wall channel, as shown in Figure 3.6.

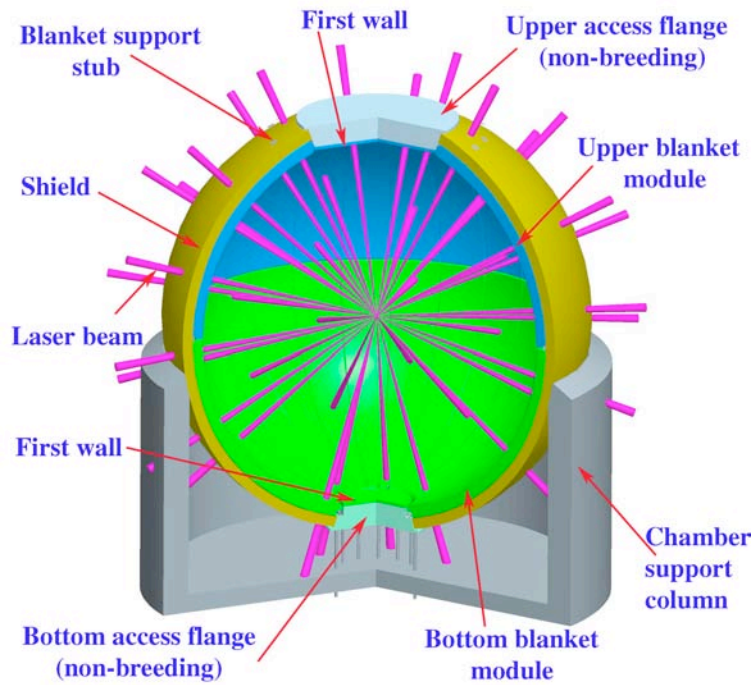


Figure 3.4 Schematic of overall chamber layout

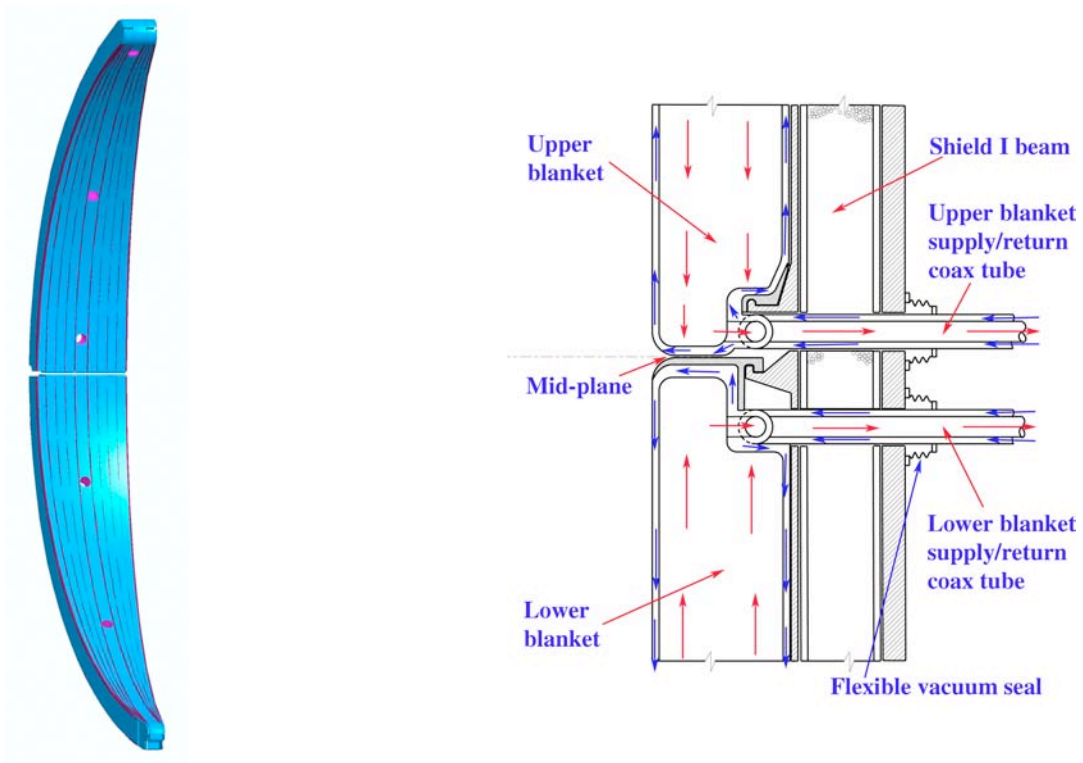


Figure 3.5 (a,b) Blanket modules including detailed of the lithium flow and supply/return tubes at midplane for the upper module.

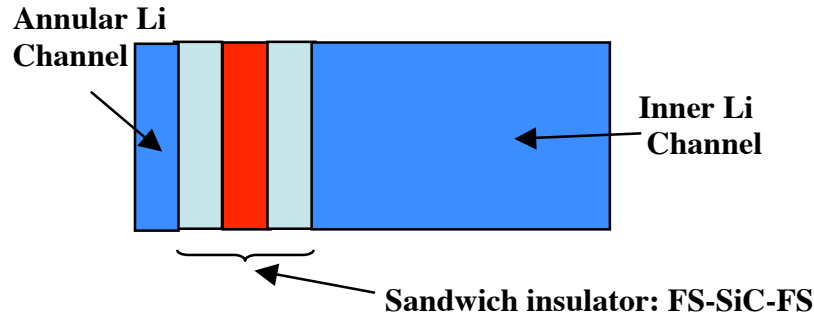


Figure 3.6 Schematic illustrating sandwich insulator region in inner wall of Li blanket module.

Two cases are considered based on material constraints approved by the MWG:

1. A baseline case with reduced activation ferritic steel (RAFS) and no corrosion coating with minimum risk in getting there based on present day material development and knowledge (focus of study).
  - Max. FW FS temp. < 550°C
  - Max. FS/Li interface temp. < 560°C (in blanket); < 575°C (outside blanket)
  
2. An advanced case with ODS-FS and corrosion coating with higher development risk (and probably higher cost also) as an indication of what could be gained with a more ambitious material R&D program.
  - Max. FW FS temp. < 700°C
  - Max. FS/Li interface temp. < 800°C

The results of the analysis for these two cases are summarized in Table 1 for cases with rep rates of 5 and 10, respectively (see publications 3.P.5 and 3.P.6, and HAPL workshop presentation 3.W. 4 for more details). The cycle efficiency is about the same for both rep rates; the pressure drop and pumping power are higher for the higher rep rate case based on the need for better coolant heat transfer to accommodate the maximum material temperature constraints but probably still acceptable. The maximum armor temperature and thermal stresses are also not affected by the rep rate provided the temperature reaches quasi steady state for the given time between shots. A major effect, however, is a reduction in component lifetime at higher rep rate as the material dpa's increase in proportion to the fusion power (or rep rate for a given yield). Other factors must also be considered (such as the target flight time and time required between shots for target injection, and the impact of higher fusion power on out of reactor component requirements and cost) before deciding on a final rep rate value.

Table 1 Summary of chamber and blanket parameters for several example cases

Yield (MJ)	350			
W armor thickness (m)	0.001			
FS front wall thickness (m)	0.0035			
Insulator sandwich layer thickness (m)	0.002			
Submodule average toroidal dimension (m)	0.205			
Submodule average radial dimension (m)	0.53			
Sandwich insulator k (W/m-K)	0.5			
	Baseline Case	Baseline Case	Advanced Case	Advanced Case
	RAFS	RAFS	ODS FS	ODS FS
Chamber radius, Rchamb (m)	10.5	10.5	11	11
Rep rate	5	10	5	10
Fusion Power (MW)	1750	3500	1750	3500
Brayton power cycle efficiency	0.37	0.37	0.49	0.49
Li Inlet temperature (C)	400.19	400.19	534.97	534.97
Li outlet temperature (°C)	575.00	575.00	800.00	800.00
Annular flow (including FW) outlet temp. (°C)	476.36	469.50	662.02	646.47
FW Li channel dimension (m)	0.0025	0.0025	0.0039	0.0025
Average velocity in FW channel (m/s)	1.82	3.64	0.75	2.36
Approx.FW FS Tmax (°C)	523.71	561.32	709.64	731.48
Approx. FW FS radial Tavg at Tmax location (°C)	503.03	519.95	690.80	693.79
Approx. pre-shot W Tmax (°C)	527.49	568.88	713.09	738.37
Max. W armor (°C)	< 2400	< 2400	< 2400	< 2400
Average velocity in inner channel(m/s)	0.072	0.143	0.047	0.093
Li/FS interface temperature at inner channel outlet (°C)	552.45	557.34	761.84	769.49
Total pressure drop (annular chan. +inner chan.) (MPa)	0.072	0.244	0.009	0.110
Total pumping power (MW)	0.453	3.054	0.037	0.940

### 3.2.3 Magnetic Intervention

The above-mentioned strategy with no protective chamber gas results in a fairly large chamber to ensure armor survival (~10.5-11 m for a target yield of 350 MJ). A parallel effort is underway to explore ways of rendering the overall concept more attractive based on size, design and performance. A possible option, as proposed by Robson [3.3], is to use magnetic intervention through a cusp field configuration in order to steer the ions (representing ~25-30% of the yield energy) away from the chamber wall. This can dramatically reduce the peak surface temperature of the chamber wall because of all the threats to the wall, the ions are the greatest contributors to the wall temperature. This would allow for more robust choices for the chamber armor as the ions can be directed to external collector plates, as illustrated in Figure 3.7. However, issues associated with the design and size of the plates as well as the magnetic field impact on the design complexity and choice of coolant must be addressed. Magnetic diversion also opens up the attractive possibility of trying to convert the ion energy to electricity with much better efficiency than that obtained by conventionally transferring the ion energy to a power cycle fluid through a heat exchanger. Since the recycling power to the laser represents a high fraction of the electrical output from a conventional power plant (up to ~25%), this would help in improving the overall plant efficiency appreciably. This seems to be the most attractive option, which needs to be further studied to better understand its attractiveness and address the key issues impacting the design.

Preliminary results on the study of this concept were presented at HAPL workshops (see presentations 3.W.1 and 3.W.5) and at the IFSA-2005 conference (see paper 3.P.4). Such a scheme gives rise to challenging issues but the potential benefit is large and warrants further study.

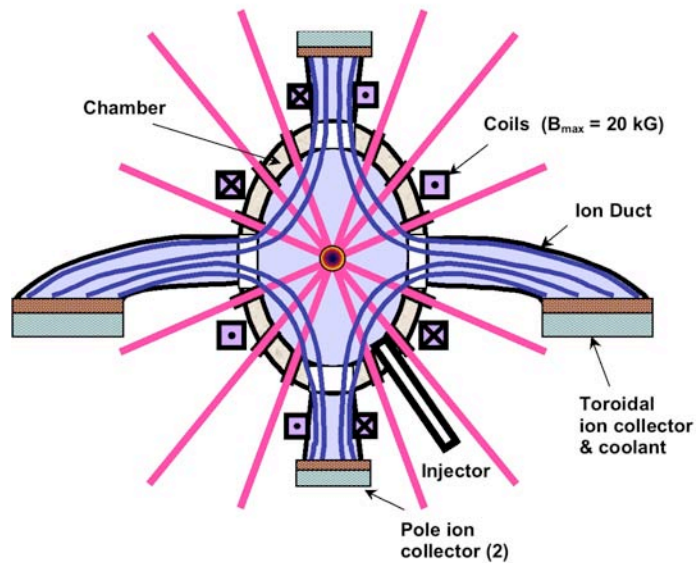


Figure 3.7 Schematic of external ion collector plates.

### References for Task 3

- 3.1 L. Snead, et al., "Refractory armored first wall development," presented at the US/Japan Workshop on Laser IFE, General Atomics, San Diego, CA (March 2005), available at: <http://aries.ucsd.edu/LIB/MEETINGS/0503-USJ-LIFE/program.shtml>.
- 3.2 G. E. Lucas and N. Walker, "IFE Ion Threat Spectra Effects Upon Chamber Wall Materials," presented at the 5<sup>th</sup> High Average Power laser Program Workshop, Naval Research Laboratory, Washington, DC (December 2002). available at: <http://aries.ucsd.edu/HAPL/MEETINGS/0212-HAPL/program.html>.
- 3.3 A. E. Robson, "Physics of, and rationale for magnetic intervention," presented at the HAPL meeting, Livermore CA, 20-21 June 2005. available at <http://aries.ucsd.edu/HAPL/MEETINGS/0506-HAPL/program.html>

## **4. Task 4: Chamber Dynamics & Clearing**

### **4.1. Statement of Purpose**

Our research aims at developing a fully integrated computer code to simulate and study the dynamic behavior of a laser-IFE chamber, including: the hydrodynamics; the effects of various heat sources and transfer mechanisms such as photon and ion heat deposition and chamber gas conduction, convection, and radiation; the chamber wall response and lifetime; and cavity clearing.

### **4.2. Progress Report**

We have developed the SPARTAN simulation code. The code solves 2-D transient compressible Navier Stokes equations. Consistent with our goal of utilizing existing computational fluid dynamics capabilities and based on discussions with several specialists in the field, the code utilizes a state-of-the-art CGF solver package (after Colella, Glaz, and Ferguson) that is based on a second-order shock-capturing Godunov scheme. It consists of a robust algorithm for compressible Euler equations and is second-order accurate in regions of smooth flow capturing shocks with a minimum of numerical dissipation and overshoot. The CGF algorithm was modified to account for dissipative terms such as viscosity. The code handles arbitrary two-dimensional geometries and includes automatic mesh refinement (AMR) techniques to speed up execution substantially. This AMR technique has been quite successful in reducing the run time of SPARTAN from a couple of weeks to several hours.

Some significant accomplishments in the last period include:

- a. Inclusion of cylindrical symmetry in SPARTAN. Simulation of the chambers with both Cartesian and cylindrical symmetry has given us the confidence that almost all 3-D effects are recovered with 2-D simulations.
- b. Inclusion of radiation from background gas that is superheated by target explosion. Because of high chamber temperature and the presence of ionized gas, chamber cooling by radiation was found to be critically important.
- c. We have assessed the effect of penetrations (e.g., laser beam ports) on the chamber gas behavior including the chamber constituents' interaction with mirrors at the end penetration lines.
- d. We have assessed different buffer gas instead of Xe and operation at different initial conditions.
- e. We have assessed chamber clearing and dynamics for a range of buffer gas pressures.

In addition, we are in the process of expanding the capability of SPARTAN to multi-species and incorporation of an aerosol model. These are expected to be completed by March 2006, the end of current contract period. Our publications under this task include:

#### References for Task 4:

- 4.1 Z. Dragojlovic and F. Najmabadi, "Simulation of IFE Chamber Dynamics Response by a Second Order Godunov Method with Arbitrary Geometry," *Proc. International Symposium on Inertial Fusion Science and Applications, IFSA 2003* (Monterey, CA, September 2002), IFSA 2003, American Nuclear Society, 850-853, 2004.
- 4.2 Z. Dragojlovic and F. Najmabadi, "Effects of Chamber Geometry and Gas Properties on Hydrodynamic Evolution of IFE Chambers," *Fusion Science & Technology*, **47**, 1152-1159 (2005).
- 4.3 Z. Dragojlovic, F. Najmabadi, and M. Day, "An Embedded Boundary Method for Viscous, Conducting Compressible Flow," Accepted for Publication, *Journal of Computational Physics* (2006).